THE JOURNAL OF BIOLOGICAL CHEMISTRY VOL. 286, NO. 43, pp. 37379–37388, October 28, 2011
© 2011 by The American Society for Biochemistry and Molecular Biology, Inc. Printed in the U.S.A.

Identification of a Molecular Activator for Insulin Receptor with Potent Anti-diabetic Effects*[S]

Received for publication, April 12, 2011, and in revised form, August 9, 2011 Published, JBC Papers in Press, September 9, 2011, DOI 10.1074/jbc.M111.247387

Kunyan He[‡], Chi-Bun Chan[‡1], Xia Liu[‡], Yonghui Jia[§], Hongbo R. Luo[§], Stefan A. France[¶], Yang Liu[‖], W. David Wilson[‖], and Keqiang Ye[‡2]

From the [‡]Department of Pathology and Laboratory Medicine, Emory University School of Medicine, Atlanta, Georgia 30322, the [§]Department of Pathology and Lab Medicine, Harvard Medical School and Children's Hospital, Boston, Massachusetts 02115, the [¶]School of Chemistry and Biochemistry, Georgia Institute of Technology, Atlanta, Georgia 30332-0400, and the [‖]Department of Chemistry, Georgia State University, Atlanta, Georgia 30033

Insulin exerts its actions through the insulin receptor (IR) and plays an essential role in diabetes. The inconvenient daily injection and undesirable side-effects associated with insulin injection demand novel drugs for the diseases. To search for bioactive insulin mimetics, we developed an *in vitro* screening assay using phospho-IR ELISA. After screening the small molecule chemical libraries, we have obtained a compound (5,8-diacetyloxy-2,3-dichloro-1,4-naphthoquinone) that provokes IR activation by directly binding to the receptor kinase domain to trigger its kinase activity at micromolar concentrations. This compound selectively activates IR but not other receptors and sensitizes insulin's action. Moreover, it elevates glucose uptake in adipocytes and has oral hypoglycemic effect in wild-type C57BL/6J mice and *db/db* and *ob/ob* mice without demonstrable toxicity. Hence, this promising compound mimics the biological functions of insulin and is useful for further drug development for diabetes treatment.

Type 2 diabetes mellitus is a heterogeneous disease that results from defective insulin actions and secretions. Various pharmacological agents are used to improve glucose homeostasis via different modes of action: sulfonylureas stimulate insulin secretion, biguanides (*e.g.* metformin) promote glucose utilization and reduce hepatic-glucose production, α-glucosidase inhibitors (*e.g.* acarbose) slow down carbohydrate absorption from the gut, and thiazolidinediones enhance cellular insulin action on glucose metabolism (1). Insulin replacement therapy is also needed when insulin production declines in the patients with poor glycemic control (2). In recent years, treatment strategies have focused on the development of novel therapeutic options to substitute insulin therapy. Several small compounds like demethylasterriquinone-B1 and TLK19780 have been identified as the functional insulin mimetics; however, they have poor bioavailability or low receptor specificity (3–5). Therefore, the search for new orally active insulin mimetics with stringent receptor selectivity is highly warranted.

In this report, we demonstrate that the naphthoquinone derivative 5,8-diacetyloxy-2,3-dichloro-1,4-naphthoquinone (DDN)[3] is a highly selective IR activator that interacts directly with the IR tyrosine kinase domain to induce Akt and ERK phosphorylations. It is also an insulin sensitizer that enhances insulin's action to stimulate glucose uptake. Oral administration of this compound robustly decreases blood glucose in wild-type and diabetic *ob/ob* and *db/db* mice. Therefore, DDN is a bioactive insulin mimetic with hypoglycemic activity.

EXPERIMENTAL PROCEDURES

Animals—Male C57BL/6J mice, male C57BL/KsJ *db/db* mice, and female C57BL/KsJ *ob/ob* mice were obtained from the Jackson Laboratory. Adult animals aged 10–12 weeks were used. Mice were housed in environmentally controlled conditions with a 12-h light/dark cycle and had free access to standard rodent pellet food and water. The animal protocols were approved by the Institutional Animal Care and Use Committee of Emory University. Animal care was given in accordance with institutional guidelines.

Cells and Reagents—CHO-IR cells (a gift from Dr. Nicholas Webster, University of California at San Diego) were maintained in Ham's F-12 plus 10% fetal bovine serum (FBS), 100 units of penicillin-streptomycin, and 200 ng/ml of G-418. NIH 3T3-L1 cells were maintained in DMEM with 10% calf bovine serum (CBS) and 100 units of penicillin-streptomycin. HEK293, and mouse embryonic fibroblast (MEF) cells were maintained in DMEM with 10% FBS and 100 units of penicillin-streptomycin. All cells were maintained at 37 °C with 5% CO_2 atmosphere in a humidified incubator. For experiments, cells were treated in the appropriate serum-free media containing compounds dissolved in DMSO. Control cells received equivalent amounts of DMSO, and the final concentration of DMSO was always kept below 0.1%. DDN was from InterBioscreen. Insulin, IGF-1, and glutathione *S*-transferase (GST)-horseradish peroxidase were from Sigma. [2-^{3}H]Deoxyglucose was pur-

* This work was supported, in whole or in part, by National Institutes of Health Grant CA127119 from NCI (to K. Y.).

[S] The on-line version of this article (available at http://www.jbc.org) contains supplemental Figs. S1 and S2 and Table S1.

[1] To whom correspondence may be addressed: Dept. of Pathology and Laboratory medicine, Emory University School of Medicine, Atlanta, GA 30322. Tel.: 404-712-2814; Fax: 404-712-2979; E-mail: cbchan@emory.edu.

[2] To whom correspondence may be addressed: Dept. of Pathology and Laboratory medicine, Emory University School of Medicine, Atlanta, GA 30322. Tel.: 404-712-2814; Fax: 404-712-2979; E-mail: kye@emory.edu.

[3] The abbreviations used are: DDN, 5,8-diacetyloxy-2,3-dichloro-1,4-naphthoquinone; IRKT, intracellular kinase domain of IR; MEF, mouse embryonic fibroblast; IGF-1R, insulin-like growth factor-1 receptor; CSN, 2,3-bismethylsulfanyl-1,4-naphthoquinone; $2NH_2$-NQ, 2-amino-1,4-naphthoquinone; ATPγS, adenosine 5′-*O*-(thiotriphosphate); IRS-1, insulin receptor substrate 1.

chased from PerkinElmer. Anti-IR β subunit and anti-IRS-1 were from Santa Cruz Biotechnology. Anti-phospho-Akt 473, anti-phospho-Erk, and anti-phospho-IR-1146 were from Cell Signaling. Anti-phosphotyrosine (pY20) and anti-phospho-IR-1158/1162/1163 were from BD Bioscience and Invitrogen, respectively. GST- intracellular kinase domain of IR (IRTK) and His-IR were from Invitrogen and R&D, respectively. All other reagents not mentioned were purchased from Sigma.

Cell-based Screening—CHO-IR cells were seeded in a 96-well plate with 15,000 cells per well in 100 μl of 0.1% FBS medium. Cells were incubated overnight, followed by 15-min treatment with 10 μM compounds in DMSO (10 mM stock concentration from the Spectrum Collection Library) at 37 °C. Control wells received vehicle or 100 nM insulin. Cells were lysed, and the phosphorylated receptors were captured with pY20 that was immobilized on ELISA plates. Bound receptors were washed then detected using an anti-IR β antibody, followed by a horseradish peroxidase-conjugated secondary antibody and colorimetric detection with 3,3′,5,5′-tetramethylbenzidine.

IR Activation by Insulin Mimetic Compounds—Cells were growth in 0.1% FBS medium overnight and then stimulated with different concentrations of drugs or insulin (100 nM), and the whole cell extracts were analyzed by immunoblotting. After a 12-h fasting, mice were orally administrated with 20 mg/kg (C57BL/6J) or 5 mg/kg (ob/ob and db/db) DDN in 0.5% methylcellulose and sacrificed at 3, 4, and 5 h following drug administration. Liver and muscle tissues were dissected quickly and frozen on dry ice. Tissue lysates were prepared and analyzed.

IR in Vitro Kinase Assay—Recombinant GST-IRTK was incubate with 50 mM Tris-HCl (pH 7.4), 10 mM $MgCl_2$, and 50 μM ATP with different concentrations of DDN for 15 min at 25 °C. Histone H2B (0.35 μg/ml) and [γ-^{32}P]ATP (0.25 μCi/μl) were added, and the samples were further incubated for 10 min. The sample was separated on a SDS-polyacrylamide gel and autoradiographed.

Partial Proteolysis Assay—200 ng of GST-IRTK was subjected to limited trypsin digestion in the presence or absence of 50 μM DDN with 50 mM Tris-HCl (pH 8.2) and 20 mM $CaCl_2$. The sample was separated on a SDS-polyacrylamide gel and stained by silver.

UV-absorption Spectra—UV-visible absorption measurement is a simple method that is applicable for exploring structural change and for knowing complex formation (6, 7). In the present study, UV-visible absorption for protein binding was obtained using the Cary 300 UV-visible spectrophotometer (Varian Inc., Palo Alto, CA) equipped with 1.0-cm quartz cells. The spectra were scanned from 200 to 800 nm in Tris buffer (0.01 M Tris, 0.05 M NaCl, 10 mM $MgCl_2$, pH 7.8). During the spectrophotometric titrations, protein (GST or GST-IRTK) was added to a cell containing a constant amount of compound. The absorbance at 602 nm was recorded (data were read three times, and mean value was obtain by averaging); the obtained data were processed with KaleidaGraph (Synergy Software). Repeated measurements were done for all the samples, and no significant differences were observed. (The reproducibility error was <5%.) Binding results from the UV titration experiments were fit with a one-site interaction model: $r = K^*C_{free}/(1 + K^*C_{free})$, where r represents the moles of bound compound per mole of protein, K is the macroscopic binding constant, and C_{free} is the free compound concentration in equilibrium with the complex.

Insulin Competition Assay—The FITC-insulin (100 nM) was incubated with CHO or CHO-IR cells in the presence of various concentrations of DDN in binding buffer (Ham's F-12, 0.5% BSA, 20 mM HEPES (pH 8.0), and 0.1% NaN_3) overnight at 4 °C. Cells were washed three times and acquired on a FACScan, and the mean channel fluorescence of bell-shaped histograms was analyzed using the program FlowJ.

[2-^{3}H]Deoxyglucose Transport—3T3-L1 preadipocytes and MEF cells were grown in standard media. After 2 days, 3T3-L1 cells were switched to differentiation media with 1 μM dexamethasone, 10 μg/ml insulin, and 0.5 mM 3-methyl-1-isobutylxanthine for 2 days, grown in post-differentiation medium containing 10 μg/ml insulin for 5 days, and then placed in standard media. NIH 3T3-L1 adipocytes were reseeded into 12-well plates 10–12 days after differentiation. Cells in 12-well plates were rinsed three times with PBS at 23 °C and preincubated with 500 μl of KRP-HEPES buffer (131.2 mM NaCl, 4.71 mM KCl, 2.47 mM $CaCl_2$, 1.24 mM $MgSO_4$, 2.48 mM NaH_2PO_4, 10 mM HEPES, and 0.5% BSA (pH 7.45)) containing insulin for 15 min or DDN for 30 min at 37 °C. The transport reaction was initiated by adding 2-deoxyglucose (final concentration, 100 μM) with [2-^{3}H]deoxyglucose (0.2 μCi/well). After 10-min incubation, cells were washed three times with ice-cold PBS and solubilized in 1% SDS, 1 M NaOH. After neutralization, radioactivity was measured by scintillation counting.

Blood Glucose Level Test—After a 12-h fasting, C57BL/6J and *db/db* mice were bled from the tail vein for a baseline (time 0) measurement with a glucometer (Accu-Chek, Roche Diagnostics). Afterward, animals were orally administered 20 mg/kg (C57BL/6J) or 5 mg/kg (*db/db*) DDN in 0.5% methylcellulose through a feeding needle. Blood glucose levels were measured at the indicated time points.

Intraperitoneal Glucose Tolerance Test—After a 12-h fasting, *ob/ob* mice were bled from the tail vein for a baseline (time, −60 min) measurement. Then animals were orally administered 5 mg/kg DDN in 0.5% methylcellulose through a feeding needle. One hour after the drug administration, glucose was administrated intraperitoneally (2 g/kg). Blood glucose levels were measured 0, 30, 60, 90, 120, and 180 min after administration of glucose. The blood was collected in tubes and kept at 4 °C overnight, and plasma was prepared by centrifugation (2000 × *g*, 20 min). Plasma insulin was measured by ELISA with a rat insulin kit (Crystal Chem). Insulin was quantified using the insulin standard curve.

Statistic Analysis—Results were expressed as mean ± S.E. from at least three independent experiments and were considered significant when p was <0.05. Statistic analysis was performed by using PRISM (GraphPad).

RESULTS

DDN and CSN Activate IR and Insulin-mediated Signaling Cascades—To search for small compounds that can rapidly activate IR, we have developed a cell-based ELISA assay using an IR stably transfected CHO-IR cell line. We seeded the cells in a 96-well plate and treated the cells with 10 μM (15 min) com-

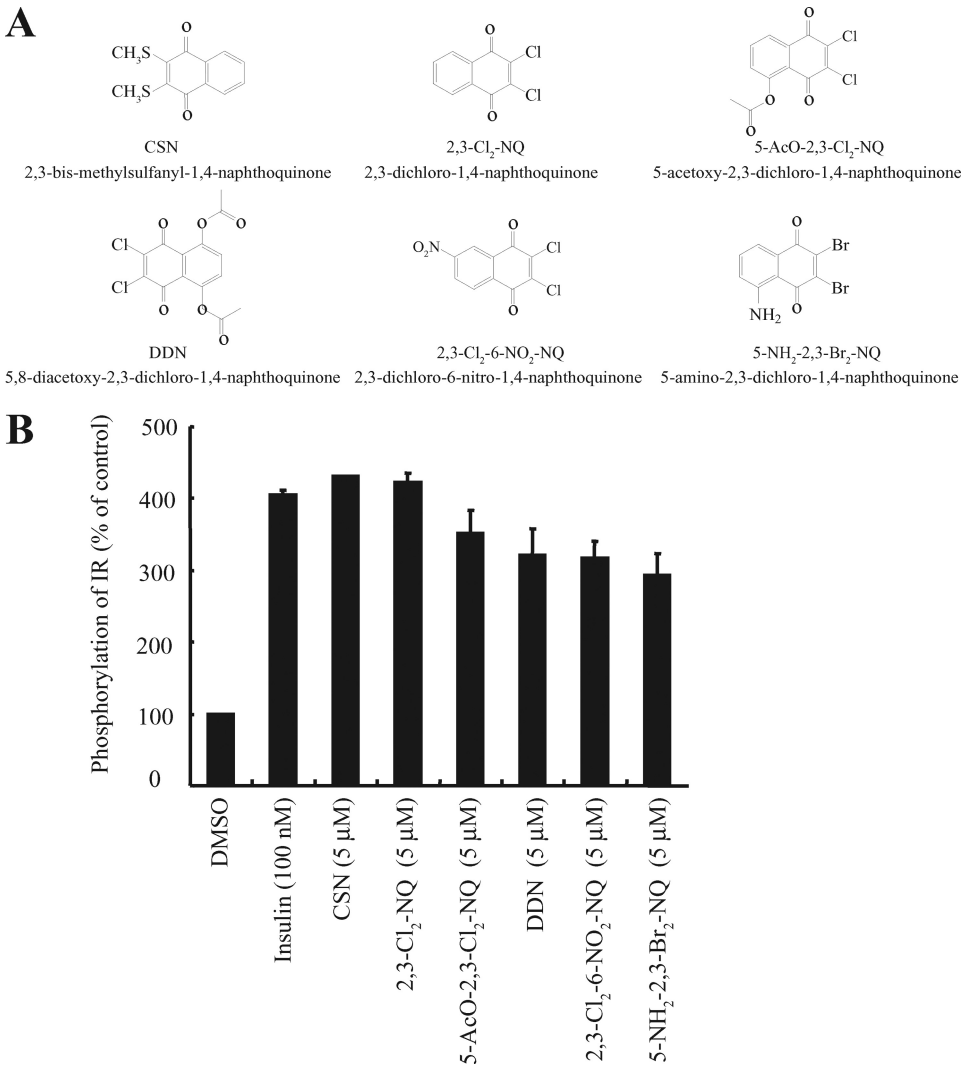

FIGURE 1. **Identification of novel insulin mimetics.** *A*, chemical structures of six compounds of 1,4-naphthoquinone derivatives. *B*, effects 1,4-naphthoquinone derivatives on IR phosphorylation in CHO-IR cells. CHO-IR cells were treated with different 1,4-naphthoquinone derivatives (5 μM) or insulin (100 nM) for 15 min. The amount of phosphorylated IR receptors was quantified by sandwich ELISA using immobilized anti-phosphotyrosine antibodies (pY20) anti-IR antibody. The activities of tested compounds were expressed as a percentage of the vehicle (DMSO) ($n = 3$).

pounds from several chemical libraries containing ~4500 natural products and synthetic chemicals. The cell lysates were subjected to the sandwich ELISA using immobilized anti-phosphotyrosine antibody and anti-IR antibody. The positive hits were subsequently analyzed on CHO-IGF-1R cells, and only the compounds that failed to activate IGF-1R were chosen for further study. Among the positive hits, we identified six 1,4-naphthoquinone compounds that can selectively activate IR but not IGF-1R (Fig. 1*A*). ELISA results revealed that all these compounds could significantly induce IR phosphorylation (Fig. 1*B*). Surprisingly, immunoblotting analysis demonstrated that only 2,3-bismethylsulfanyl-1,4-naphthoquinone (CSN) and DDN strongly stimulated tyrosine phosphorylation of the IR β subunit in Tyr-1146 (Fig. 2*A*, *first panel*) and Tyr-1158/1162/1163 (Fig. 2*A*, *second panel*). Total IR tyrosine phosphorylation was further confirmed by immunoprecipitation using anti-phosphotyrosine (pY20) antibody (Fig. 2*A*, *third panel*). Presumably, the discrepant IR phosphorylation levels between ELISA and immunoblotting assay were caused by nonspecific signal and a low detection limit of the ELISA. Consistent with IR activation, the tyrosine phosphorylation of IRS-1 of CHO-IR cells was also increased when stimulated by both DDN and CSN (Fig. 2*A*, *fifth panel*). A titration assay showed both compounds activated IR in a dose-dependent manner. At 5 μM, both compounds evidently stimulated IR phosphorylation and downstream Akt and ERK activation in a dose-dependent manner (Fig. 2*B*). The time-course assay demonstrated that CSN activated IR in CHO-IR cells at 5–15 min, peaked at 60 min, and the signal decreased at 2 h (Fig. 2*C*, *middle panel*). In contrast, significant IR phosphorylation started 5 min after DDN stimulation, and the signals escalated with the time course (Fig. 2*C*, *right panel*). Although insulin activated IR signaling at 0.05 μM, these compounds stimulated the IR signal cascades at 5 μM (Fig. 2*D*). Neither IGF-1R nor EGFR was activated by any of these compounds even at 10 μM, underscoring that these molecules possess selectivity toward different receptors (Fig. 2*E*). Hence, both DDN and CSN potently and specifically stimulate IR and its downstream signaling cascades in intact cells.

DDN Displays Hypoglycemic Effect in Mice—To explore whether DDN and CSN can mimic insulin in provoking IR and

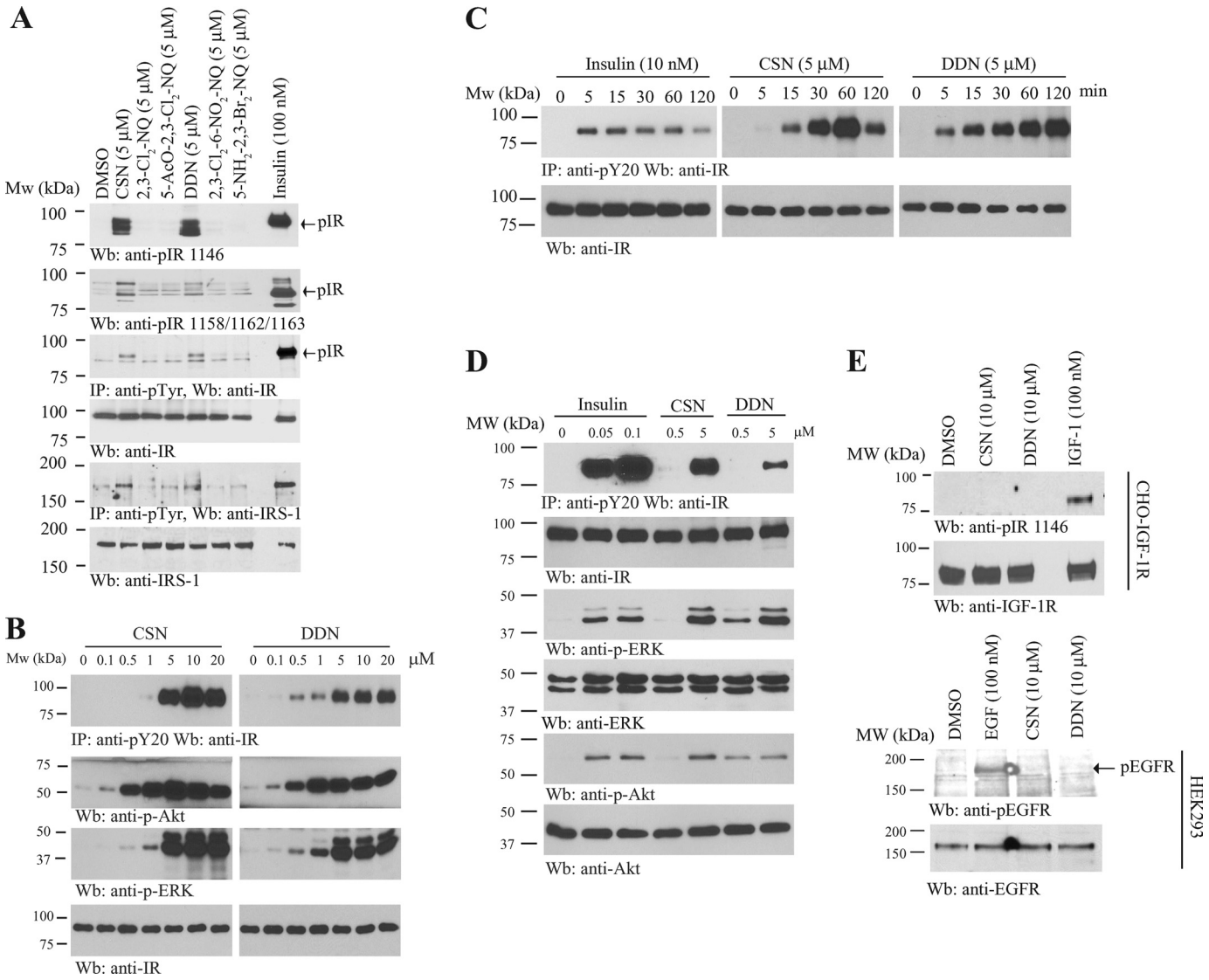

FIGURE 2. **DDN and CSN activate IR and its downstream signaling.** *A*, DDN and CSN activate IR and its downstream signaling in CHO-IR cells. CHO-IR cells were treated with insulin (100 nM) or various 1,4-naphthoquinone derivatives (5 μM) for 15 min. The cell lysates were analyzed by immunoblotting with anti-phospho-IR antibodies, or immunoprecipitated by pY20 and analyzed using anti-IR and anti-IRS-1, respectively. *B*, DDN and CSN induce IR phosphorylation in a dose-dependent manner. CHO-IR cells were treated with the small compounds at different concentrations for 15 min, and the IR phosphorylation was monitored by immunoprecipitation and immunoblotting. *C*, DDN and CSN induce IR phosphorylation in a time-dependent manner. CHO-IR cells were treated with DDN (5 μM), CSN (5 μM), and insulin (10 nM) for various times, and the IR phosphorylation was monitored by immunoprecipitation and immunoblotting. *D*, DDN and CSN induce IR phosphorylation and its downstream signaling in a dose-dependent manner. CHO-IR cells were treated with various concentrations of DDN or CSN for 30 min, or insulin for 15 min, and the IR phosphorylation and its downstream signaling were monitored by immunoprecipitation and immunoblotting. *E*, DDN and CSN cannot induce IGF-1R or EGFR phosphorylation. CHO-IGF-1R or HEK293 cells were treated with EGF (100 nM), IGF-1 (100 nM), DDN (10 μM), or CSN (10 μM) for 15 min. The cell lysates were analyzed by immunoblotting with anti-pIGF-1R and anti-pEGFR.

its downstream IRS-1 activation *in vivo*, we intraperitoneally administrated various doses of DDN and CSN into C57BL/6J mice. However, CSN was lethal to the mice even at low doses (1 mg/kg) (data not shown). Hence, we only focused on DDN for the subsequent experiments. We tested if DDN possesses hypoglycemic functions. After oral injection, DDN significantly reduced blood glucose in C57BL/6 mice as compared with vehicle control. The kinetics of DDN in lowering blood glucose is different from that of insulin. Thirty minutes after intraperitoneal injection of insulin, the blood glucose concentration was reduced; however, a significant decrease of blood glucose could only be detected after 3 h of DDN administration. On the other hand, injection of the inactive analog 2-amino-1,4-naphthoquinone ($2NH_2$-NQ) at the same dosage had no effect (see Fig. 3*A* for the percentage change and supplemental Fig. S1 for the absolute blood glucose concentrations). To monitor the IR signaling cascades in insulin-sensitive tissues, we injected 20 mg/kg DDN into C57BL/6J mice via oral gavage, sacrificed the animals at different time points, and monitored IR tyrosine phosphorylation by immunoblotting. In liver and muscle, DDN elicited demonstrable IR activation after 3–4 h (Fig. 3*B*, *first panel*). Immunoprecipitation using pY20 antibody also confirmed IRS-1 tyrosine phosphorylation in both tissues after stimulated by DDN (Fig. 3*B*, *third panel*); in contrast, DDN did not stimulate IGF-IR activation in either muscle or liver (Fig. 3*B*, *fifth panel*), which concurred with our *in vitro* observation (Fig. 2*E*). Neither IR nor IRS-1 phosphorylations were increased after $2NH_2$-NQ injection (Fig. 3*B*). To test whether

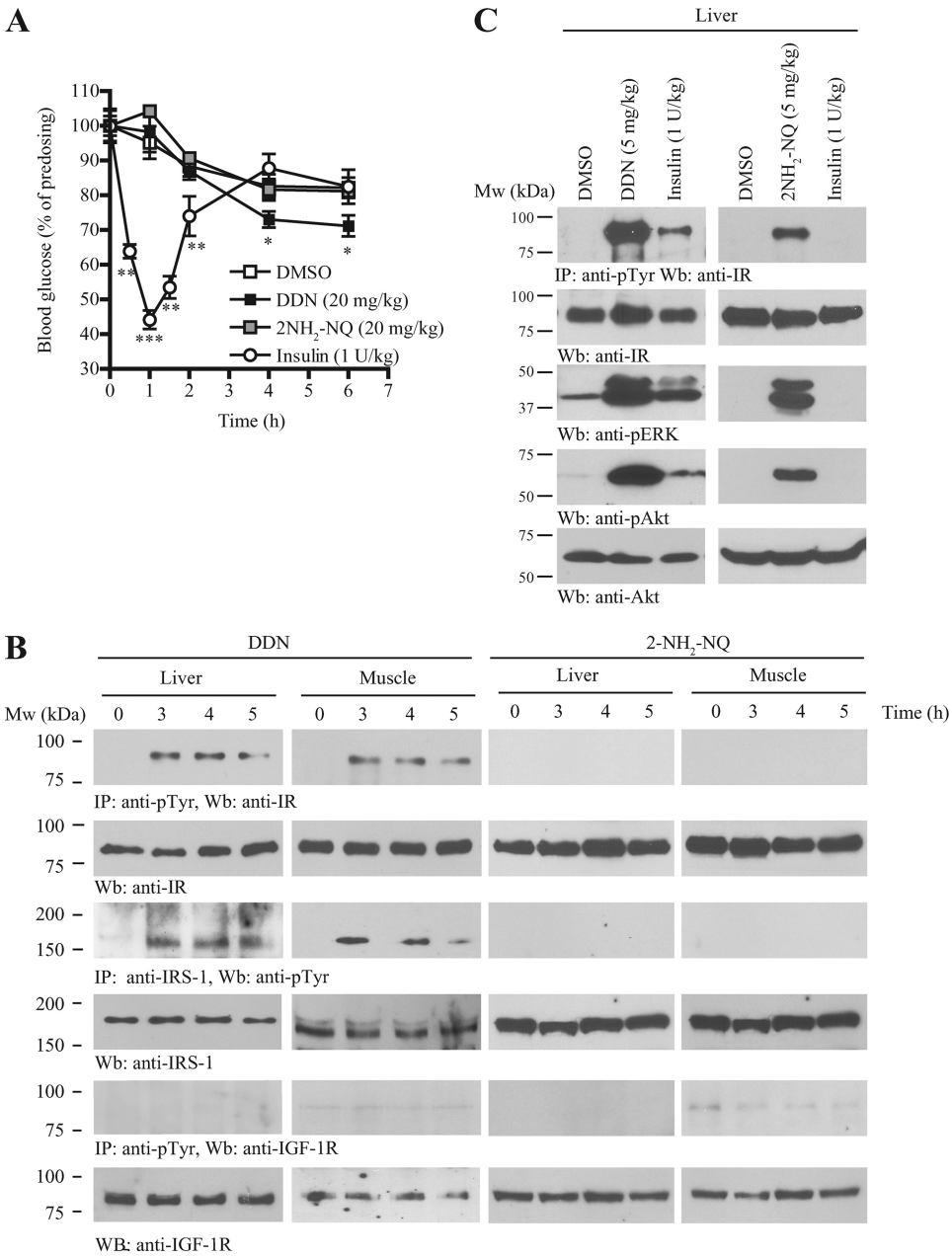

FIGURE 3. **DDN activates insulin signaling pathways *in vivo* and possesses hypoglycemic activity.** *A*, DDN reduces blood glucose in C57BL/6J mice. C57BL/6J mice were starved for 12 h and then orally administrated with vehicle (0.5% methylcellulose), DDN (20 mg/kg), or the inactive analog $2NH_2$-NQ (20 mg/kg). Human insulin (1 unit/kg) was injected intraperitoneally as a positive control. Blood glucose was monitored before and after dosing at various time points as indicated (*, $p < 0.05$; **, $p < 0.01$; ***, $p < 0.001$, $n = 10–13$, Two-way analysis of variance *versus* vehicle). *B*, DDN provokes IR phosphorylation and its downstream signaling in C57BL/6J mice. Three-month-old C57BL/6J mice were starved for 12 h and then orally administrated with vehicle (0.5% methylcellulose), DDN (20 mg/kg), or $2NH_2$-NQ (20 mg/kg). Cell lysates were prepared from liver and muscle tissues, which were collected at 3, 4, and 5 h after drug administration and analyzed by immunoprecipitation and immunoblotting. *C*, DDN quickly activates IR phosphorylation and its downstream signaling. Three-month-old C57BL/6J mice were starved for 12 h and then injected with vehicle, 5 mg/kg DDN, or 5 mg/kg $2NH_2$-NQ through the vena cava. After 5 min, the liver was collected and analyzed by immunoblotting using specific antibodies.

DDN has an acute effect as insulin, DDN or $2NH_2$-NQ was injected into the animal through the vena cava. The liver was then dissected and homogenized after 5 min. Immunoprecipitation using pY20 antibody demonstrated that DDN, but not $2NH_2$-NQ, quickly activated IR (Fig. 3*C*, *first panel*) and Akt and ERK (Fig. 3*C*, *third* and *fifth panels*, respectively).

Similarly to the observation in C57/BL6 mice, DDN induced IR signaling in the well established mice models of non-insulin-dependent diabetes mellitus. Oral injection of DDN enhanced IR and ERK phosphorylations in *db/db* (Fig. 4*A*) and *ob/ob* (Fig. 4*B*) mice. One hour after oral administration of DDN, lower blood glucose was found in *db/db* mice as compared with vehicle control (Fig. 4*C*). In contrast to the findings in C57/BL6 mice, the time needed for DDN to lower the blood glucose in *db/db* mice was comparable to that of insulin injection, but the effect of DDN could be sustained till the end of the experiment, whereas the effect of insulin vanished 2 h after injection. Oral administration of DDN to *ob/ob* mice also led to significant

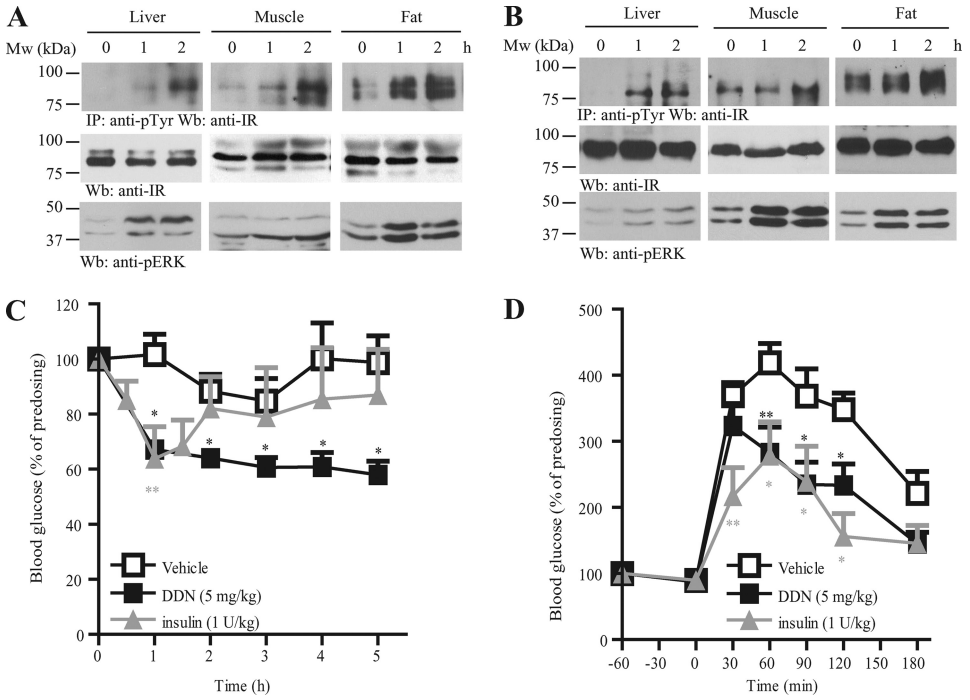

FIGURE 4. **DDN displays hypoglycemic function in diabetic mouse models.** *A*, DDN activates insulin signaling in *db/db* mice. Three-month-old mice were starved for 12 h and then orally administrated with vehicle (0.5% methylcellulose) or DDN (5 mg/kg). Cell lysates were prepared from liver and muscle tissues, which were collected at 1 and 2 h after drug administration and analyzed by immunoprecipitation and immunoblotting. *B*, DDN activates insulin signaling in *ob/ob* mice. Three-month-old mice were starved for 12 h and then orally administrated with vehicle (0.5% methylcellulose) or DDN (5 mg/kg). Cell lysates were prepared from liver and muscle tissues, which were collected at 1 and 2 h after drug administration and analyzed by immunoprecipitation and immunoblotting. *C*, hypoglycemic function of DDN in *db/db* mice. The animals were starved for 12 h and then orally injected with vehicle (0.5% methylcellulose) or DDN (5 mg/kg). Human insulin (1 unit/kg) was injected intraperitoneally as a positive control. Blood glucose was monitored before and after drug administration at 1-h intervals (*, $p < 0.05$; **, $p < 0.01$, $n = 5$; two-way analysis of variance *versus* vehicle). *D*, DDN improves the glucose tolerance in *ob/ob* mice. The animals were starved for 12 h and then orally dosed with vehicle (0.5% methylcellulose) or DDN (5 mg/kg). Human insulin (1 unit/kg) was injected intraperitoneally as a positive control. A bonus of glucose (2 gm/kg) was injected intraperitoneally 1 h later. Blood glucose was measured at 30-min intervals (*, $p < 0.05$; **, $p < 0.01$, $n = 5$; two-way analysis of variance *versus* vehicle control).

improvement in glucose tolerance, which was comparable to the effect of insulin injection (Fig. 4*D*). Nonetheless, single oral doses of DDN had no significant effect on plasma insulin levels in *ob/ob* mice (data not shown), suggesting the hypoglycemic function of DDN did not act through the change of insulin secretion.

Treatment of wild-type C57BL/6J mice ($n = 5$) with daily oral administration of DDN (5 mg/kg) for 16 days did not affect the food intake (supplemental Fig. S1) or blood biochemistry (supplemental Table S1). Pathological examination also failed to detect any demonstrable toxicity in brain, heart, liver, kidney, and muscle (data not shown), indicating that the compound might not possess any intolerable toxicity. Hence, DDN mimics insulin and effectively lowers blood glucose in wild-type and insulin-resistant *db/db* and *ob/ob* mice.

DDN Induces Cellular Glucose Uptake—The observation that DDN effectively reduced circulating glucose in animals suggested that it might enhance glucose absorption. Therefore, we examined the effect of DDN on glucose uptake in adipocytes, a well characterized cellular model for insulin-induced glucose homeostasis. Differentiated 3T3-L1 adipocytes were treated with various concentrations of DDN, and the activation of Akt was monitored. As expected, DDN elicited a dose-dependent IR and Akt activation (Fig. 5*A*). Moreover, DDN escalated [^{3}H]deoxyglucose uptake in a dose-dependent manner (Fig. 5*B*), which concurred with the Akt phosphorylation pattern.

It is noteworthy that DDN sensitized the insulin activity. In differentiated 3T3-L1 cells, 5 nM insulin was able to trigger IR phosphorylation (Fig. 5*C*, *first panel*, *lane 2*). However, DDN at the same concentration did not induce any IR activation (Fig. 5*C*, *first panel*, *lane 3*). When the two insulin and DDN were added together, IR phosphorylation was higher than those observed when insulin or DDN was administrated separately, suggesting DDN can potentiate insulin activity. Akt phosphorylation tightly correlated with the IR activity after insulin or DDN stimulation (Fig. 5*C*, *third panel*). In addition, DDN elevated insulin activity in triggering glucose uptake in differentiated 3T3-L1 cells. Consistent with the IR activation pattern, stimulation with 5 nM insulin, but not DDN, significantly increased the [^{3}H]deoxyglucose uptake in 3T3-L1 cells. When insulin and DDN were administrated together, the magnitude of glucose uptake was further increased (Fig. 5*D*).

To confirm that the DDN-induced biological effect was IR-dependent, we knocked down IR in the differentiated adipocytes using siRNA and monitored the insulin signaling. Western blot analysis showed that IR expression was significantly decreased in cells transfected with siRNA against IR (Fig. 5*E*, *first panel*). Both insulin- and DDN-triggered ERK phosphorylation were reduced when IR was depleted, underscoring that IR is the major molecular target of DDN to trigger ERK activation (Fig. 5*E*, *second panel*). We also treated phosphatidylinositol 3-kinase p85 subunit-ablated (p85$\alpha^{-/-}$) MEF with DDN and determined its glucose uptake activity. It has been

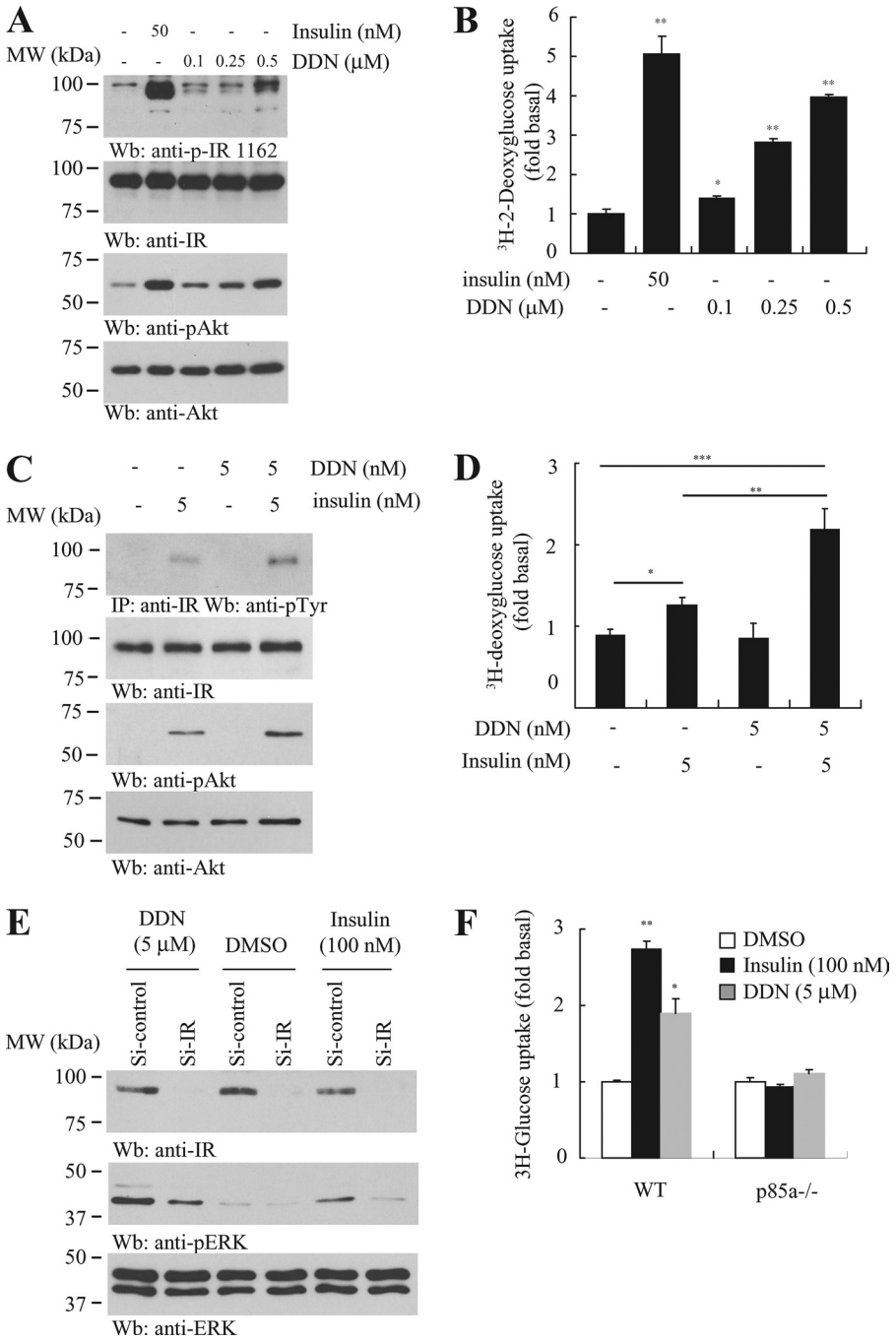

FIGURE 5. **DDN enhances cellular glucose uptake.** *A*, DDN provokes IR signaling in differentiated 3T3-L1 adipocytes. The 3T3-L1 cells were stimulated with insulin (50 nM) for 15 min or DDN (0.1, 0.25, and 0.5 μM) for 30 min. Insulin signaling in the cell lysates was tested by immunoblotting. *B*, DDN stimulates glucose uptake. Differentiated 3T3-L1 adipocytes were stimulated with insulin (50 nM) for 15 min or DDN (0.1, 0.25, and 0.5 μM) for 30 min. [2-^{3}H]Deoxyglucose was then added, and the cells were further incubated for 10 min. [2-^{3}H]Deoxyglucose uptake by adipocytes was measured by scintillation counting (*, $p < 0.05$; **, $p < 0.01$ *versus* control, Student's *t* test, $n = 3$). *C*, DDN synergizes insulin signaling. Differentiated 3T3-L1 adipocytes were stimulated with 5 nM insulin, 5 nM DDN, or a combination of the two drugs. Cell lysates were then prepared for Western blot using specific antibodies as indicated. *D*, DDN synergizes insulin activity in promoting glucose uptake. Differentiated 3T3-L1 adipocytes were stimulated with 5 nM insulin, 5 nM DDN, or a combination of the two drugs. [2-^{3}H]Deoxyglucose was then added, and the cells were further incubated for 10 min. [2-^{3}H]Deoxyglucose uptake by adipocytes was measured by scintillation counting (*, $p < 0.05$; **, $p < 0.01$, Student's *t* test, $n = 3$). *E*, IR is necessary for DDN to induce ERK phosphorylation. Differentiated 3T3-L1 adipocytes were transfected with control siRNA or siRNA against IR. The cells were then stimulated with insulin (100 nM) for 15 min or DDN (5 μM) for 30 min. Cell lysates were analyzed by Western blot. *F*, the glucose uptake induced by DDN in *p85α* knock-out MEF cells. Wild-type and *p85α*$^{-/-}$ MEF cells were treated with 100 nM insulin for 15 min or 5 μM DDN for 30 min. The uptake of [2-^{3}H]deoxyglucose was monitored by liquid scintillation counting (*, $p < 0.05$; **, $p < 0.01$ *versus* control, Student's *t* test, $n = 3$).

reported that MEFs with p85 ablation are defective in insulin-stimulated glucose uptake (8). Both insulin and DDN triggered robust [^{3}H]deoxyglucose uptake in wild-type MEF cells but not p85$\alpha^{-/-}$ cells (Fig. 5*F*), suggesting that an intact IR/phosphatidylinositol 3-kinase/Akt cascade is necessary for DDN to exert its hypoglycemic function.

DDN Binds to the Kinase Domain of Insulin Receptor—The synergistic function of DDN on insulin-induced IR activation

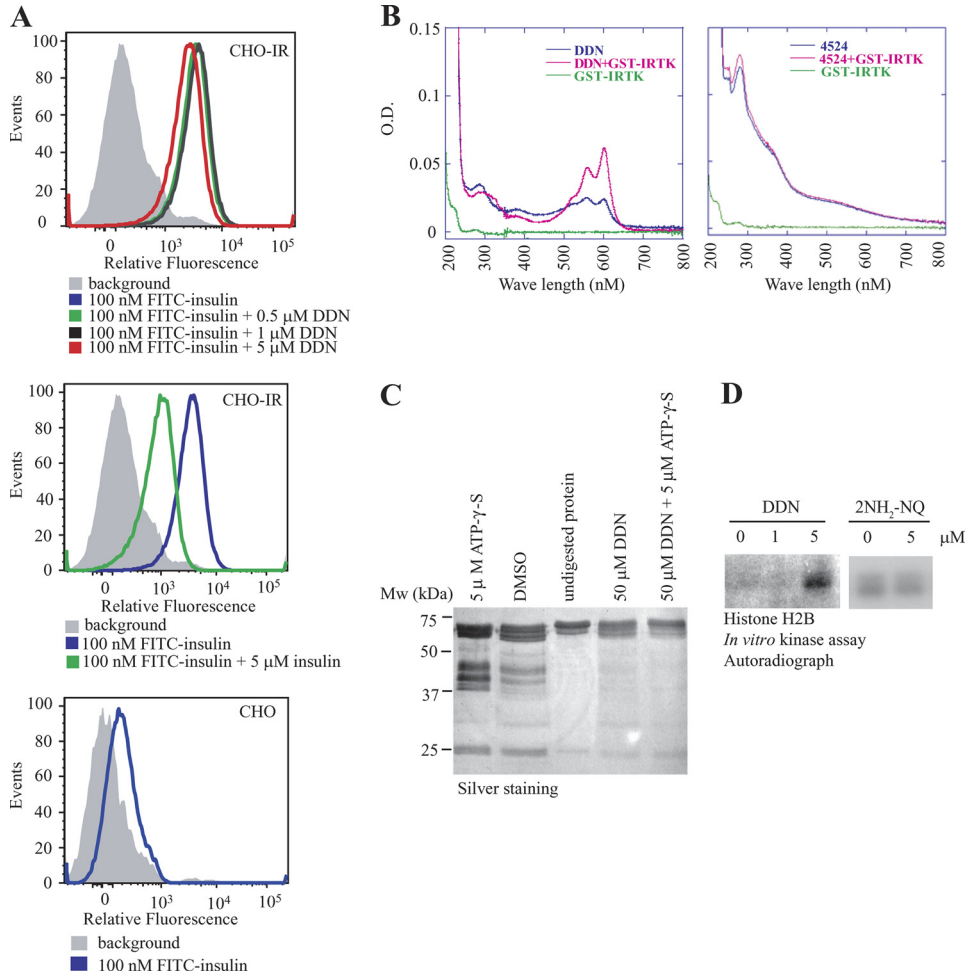

FIGURE 6. **DDN interacts and activates the insulin receptor.** *A*, DDN does not complete with insulin for IR binding site. FITC-insulin was incubated with CHO-IR cells in the presence of various concentrations of DDN (*top panel*) or unlabeled insulin (*middle panel*). Parental CHO cells were used as a negative control (*bottom panel*). The fluorescence-labeled cells were analyzed on flow cytometry. *B*, DDN binds to IRTK. UV-visible spectra were scanned from 200 to 800 nm for IRTK fragment in the presence of DDN or its analog. When DDN binds to IRTK, it elicits the absorption alteration at 560 and 602 nm. *C*, DDN protects IRTK from proteolysis. GST-IRTK was subjected to limited trypsin digestion in the presence of DDN (50 μM), ATPγS (5 mM), or both. The reaction mixture was resolved by SDS-PAGE, followed by silver staining. *D*, DDN increases IRTK activity *in vitro*. Recombinant GST-IRTK was incubated with different concentrations of DDN or its inactive analog $2NH_2$-NQ, and the kinase activity of IRTK was examined by monitoring the phosphorylation of histone H2B using autoradiography.

suggests that insulin and DDN might share differential IR binding sites. We therefore performed insulin competition assay using flow cytometry (9). CHO-IR cells were incubated with 100 nM FITC-insulin in the presence of DDN at different concentrations. The binding of FITC-insulin to the cell surface IR increased the fluorescent signal of CHO-IR cells, leading to a right shift of the peak. No significant change of the shifted peak position was observed in the presence of DDN (Fig. 6*A*, *top panel*). However, a left shift of the fluorescent peak was detected, when 5 μM unlabeled insulin was added, suggesting a successful competition between unlabeled insulin and FITC-insulin for the ligand binding (Fig. 6*A*, *middle panel*). As a negative control, FITC-insulin did not bind to the IR-deficient parental CHO cells (Fig. 6*A*, *bottom panel*). These results suggest that DDN and insulin might possess different ligand binding sites on IR.

Several small molecules bind to IRTK and provoke its activation (3–5). Thus, DDN might also interact with the IRTK to activate IR. To test this possibility, we performed an UV-absorption spectra analysis using recombinant IRTK. Although the GST-tagged IRTK (GST-IRTK, amino acids 1011–1382) had no absorption from 200 to 800 nm, addition of DDN, but not its structural related analog, naptho[2,3-*d*]thiazole-4,9-dione-2-[(4-chlorophenyl)amino] enhanced the peak absorption at 560 and 602 nm (Fig. 6*B*), suggesting a specific interaction occurs between DDN and IRTK. A titration assay revealed that the binding constant K_d of DDN to GST-IRTK was ~3.27 ± 1.06 μM. We also performed the partial proteolysis analysis to confirm the DDN-IRTK interaction as previously described (4). We first incubated recombinant GST-tagged IRTK with either DMSO or DDN, followed by limited trypsin digestions. In DMSO treatment, GST-IRTK was digested into several smaller fragments of various molecular weights. However, DDN pretreatment protected IRTK against trypsin digestion with more intact IRTK observed (Fig. 6*C*). As a positive control, the presence of ATPγS also altered the proteolysis pattern. Whereas a band of ~37 kDa presented strongly in the ATPγS-incubated IRTK, a band of ~30 kDa was found in the control samples but attenuated in the ATPγS-treated sample. We further examined if DDN alters the kinase activity of IRTK through direct inter-

action by performing an *in vitro* histone phosphorylation assay (4). As expected, DDN, but not the inactive analog $2NH_2$-NQ, activated the recombinant IRTK to phosphorylate histone H2B (Fig. 6*D*). Therefore, DDN activates IR by increasing the kinase activity of IR through direct interaction.

DISCUSSION

In this report, we have identified the 1,4-naphthoquinone derivative DDN as a new small molecular IR activator *in vitro* and *in vivo*. DDN has a simple chemical structure with prominent effect in selectively provoking IR activation and lowering blood glucose in animals. Thus, it represents a novel prototype for further chemical modification to generate a powerful therapeutic drug for diabetes.

Zhang *et al.* have reported that DAQ B1 is an orally active IR ligand with anti-diabetic activity (4). Webster and his colleagues have conducted an extensive structure-activity relationship study on DAQ B1 derivatives and successfully identified the mono-indolyl-dihydroxybenzoquinones ZL-196 and LD-17, which activate IR signaling and effectively lower blood glucose in *db/db* mice (10). However, these compounds cannot selectively induce IR, and they also provoke other receptor tyrosine kinases, including IGF-1R, NGFR, and EGFR (10, 11). In contrast, DDN specifically activates IR and its downstream cascades. A few classes of non-peptidyl IR activators have also been reported with different modes of actions. For example, TLK19780 is an insulin sensitizer, which potentiates insulin-triggered IR phosphorylation (3, 12). However, it is inactive when administrated alone. We also found that DDN potentiates the action of insulin in promoting IR activation and up-regulating glucose uptake. This additive effect might be a result of differential usage of IR ligand binding sites for insulin and DDN. Indeed, we have shown that DDN does not complete with insulin for IR binding but binds to the IR kinase domain directly. Hence, IR could simultaneously interact with both insulin on its extracellular domain and DDN on its intracellular kinase domain.

When administrated orally, DDN has hypoglycemic function in both normal and diabetic mice models, and the glucose-lowering effect could be observed after 1-h administration. It is possible that the metabolites of DDN, in addition to DDN itself, might also possess the hypoglycemic activity *in vivo*. However, our cell-based *in vitro* studies showed that DDN directly bound IR and activated it within 5–15 min, suggesting DDN *per se* has a significant role in provoking IR activation. Moreover, IR activation in liver and muscle could be observed in 5 min, when DDN was injected into the bloodstream directly through the vena cava. It is interesting to note that DDN takes shorter time to reduce the blood glucose level in *db/db* mice than in normal C57BL/6 mice. One of the possible explanations is that the *db/db* mice have more adipose tissue than the normal mice, which may provide more insulin-responsive "storage sites" for the blood glucose. Thus, the *db/db* mice have more "targets" upon which DDN can exert its hypoglycemic function. Another possibility is that *db/db* mice have higher intestinal permeability (13). Because DDN is given via oral administration in the current studies, the higher absorption in the intestine of *db/db* mice thus promotes more DDN into the bloodstream, leading to a better efficacy in lowering blood glucose. It is noteworthy that a similar observation is made in the study using another quinone-based insulin mimetic Compound 2h. Compound 2h is more potent in lowing blood glucose in *db/db* mice than the lean control, suggesting that it may be a common characteristic for quinone-based insulin mimetics (11).

CSN is also an effective IR activator *in vitro*. However, it is lethal to animals when administrated *in vivo*. 1,4-Naphthoquinones are widely distributed phenolic compounds in nature, and they display diverse pharmacological properties like antibacterial, antifungal, antiviral, anti-inflammatory, and antipyretic properties, including anticancer activity (14, 15). Most of these quinoids belong to DNA-intercalating agents (16, 17). For instance, Plumbagin (5-hydroxy-2-methyl-1,4-naphthoquinone), derived from Plumbagineae and Droseraceae families, can induce mammalian topoisomerase II-mediated DNA cleavage *in vitro* (18). Therefore, they are effective anticancer agents against murine fibrosarcoma, P388 lymphocytic leukemia, and A549 non-small cell lung cancer cells (19–21). In addition, the semiquinone radicals, generated either by one-electron reduction or two-electron reduction followed by a subsequent oxidation from quinine by dehydrogenase, damage the thiol groups or nucleophilic moieties of proteins (22). The oxidative stress induced by these quinone derivatives has been proposed to be responsible for initiation of cellular damage (23). Conceivably, the metabolites of CSN may covalently modify the thiol groups in many proteins, which may lead to its adverse side-effects. In contrast, DDN does not exhibit any intolerable side-effects when administrated to animals for 2 weeks, suggesting DDN and CSN might behave very differently.

Acknowledgment—We are indebted to Dr. Nicholas Webster at the University of California, San Diego for CHO-IR and CHO-IGF-1R stable cell lines.

REFERENCES

1. Fonseca, V. A., and Kulkarni, K. D. (2008) *J. Am. Diet. Assoc.* **108,** S29-S33
2. Campbell, R. K. (2009) *J. Am. Pharm. Assoc.* **49,** Suppl. 1, S3-S9
3. Pender, C., Goldfine, I. D., Manchem, V. P., Evans, J. L., Spevak, W. R., Shi, S., Rao, S., Bajjalieh, S., Maddux, B. A., and Youngren, J. F. (2002) *J. Biol. Chem.* **277,** 43565–43571
4. Zhang, B., Salituro, G., Szalkowski, D., Li, Z., Zhang, Y., Royo, I., Vilella, D., Díez, M. T., Pelaez, F., Ruby, C., Kendall, R. L., Mao, X., Griffin, P., Calaycay, J., Zierath, J. R., Heck, J. V., Smith, R. G., and Moller, D. E. (1999) *Science* **284,** 974–977
5. Wilkie, N., Wingrove, P. B., Bilsland, J. G., Young, L., Harper, S. J., Hefti, F., Ellis, S., and Pollack, S. J. (2001) *J. Neurochem.* **78,** 1135–1145
6. Jayabharathi, J., Thanikachalam, V., and Venkatesh Perumal, M. (2011) *Spectrochim. Acta A Mol. Biomol. Spectrosc.* **79,** 502–507
7. Maiti, T. K., Ghosh, K. S., Debnath, J., and Dasgupta, S. (2008) *J. Photochem. Photobiol. A Chemistry* **194,** 297–307
8. Ueki, K., Fruman, D. A., Yballe, C. M., Fasshauer, M., Klein, J., Asano, T., Cantley, L. C., and Kahn, C. R. (2003) *J. Biol. Chem.* **278,** 48453–48466
9. Zaccaro, M. C., Lee, H. B., Pattarawarapan, M., Xia, Z., Caron, A., L'Heureux, P. J., Bengio, Y., Burgess, K., and Saragovi, H. U. (2005) *Chem. Biol.* **12,** 1015–1028
10. Lin, B., Li, Z., Park, K., Deng, L., Pai, A., Zhong, L., Pirrung, M. C., and Webster, N. J. (2007) *J. Pharmacol. Exp. Ther.* **323,** 579–585
11. Liu, K., Xu, L., Szalkowski, D., Li, Z., Ding, V., Kwei, G., Huskey, S., Moller, D. E., Heck, J. V., Zhang, B. B., and Jones, A. B. (2000) *J. Med. Chem.* **43,** 3487–3494

12. Manchem, V. P., Goldfine, I. D., Kohanski, R. A., Cristobal, C. P., Lum, R. T., Schow, S. R., Shi, S., Spevak, W. R., Laborde, E., Toavs, D. K., Villar, H. O., Wick, M. M., and Kozlowski, M. R. (2001) *Diabetes* **50,** 824–830
13. Brun, P., Castagliuolo, I., Di Leo, V., Buda, A., Pinzani, M., Palù, G., and Martines, D. (2007) *Am. J. Physiol. Gastrointest. Liver Physiol.* **292,** G518-G525
14. Kim, B. H., Yoo, J., Park, S. H., Jung, J. K., Cho, H., and Chung, Y. (2006) *Arch. Pharm. Res.* **29,** 123–130
15. Babula, P., Adam, V., Havel, L., and Kizek, R. (2007) *Ceska. Slov. Farm.* **56,** 114–120
16. Yamashita, N., Maruyama, M., Yamazaki, K., Hamazaki, T., and Yano, S. (1991) *Clin. Immunol. Immunopathol.* **59,** 335–345
17. Prasad, V. S., Devi, P. U., Rao, B. S., and Kamath, R. (1996) *Indian J. Exp. Biol.* **34,** 857–858
18. Fujii, N., Yamashita, Y., Arima, Y., Nagashima, M., and Nakano, H. (1992) *Antimicrob. Agents Chemother.* **36,** 2589–2594
19. Krishnaswamy, M., and Purushothaman, K. K. (1980) *Indian J. Exp. Biol.* **18,** 876–877
20. Singh, U. V., and Udupa, N. (1997) *Indian J. Physiol. Pharmacol.* **41,** 171–175
21. Hsu, Y. L., Cho, C. Y., Kuo, P. L., Huang, Y. T., and Lin, C. C. (2006) *J. Pharmacol. Exp. Ther.* **318,** 484–494
22. Babich, H., Stern, A., and Munday, R. (1993) *Toxicol. Lett.* **69,** 69–75
23. Smith, M. T. (1985) *J. Toxicol. Environ. Health* **16,** 665–672